Science of the Total Environment 927 (2024) 172166

Contents lists available at ScienceDirect

Science of the Total Environment

journal homepage: www.elsevier.com/locate/scitotenv

Drought legacies in mixed Mediterranean forests: Analysing the effects of structural overshoot, functional traits and site factors

Santain S.P. Italiano [a], J. Julio Camarero [b], Marco Borghetti [a], Michele Colangelo [a,b], Angelo Rita [c], Francesco Ripullone [a,*]

[a] Scuola di Scienze Agrarie, Forestali, Alimentari e Ambientali, Università della Basilicata, Viale dell'Ateneo Lucano 10, 85100 Potenza, Italy
[b] Instituto Pirenaico de Ecología (IPE-CSIC), Avda. Montañana 1005, E-50192 Zaragoza, Spain
[c] Dipartimento di Agraria, Università di Napoli Federico II, via Università 100, IT-80055 Portici, Napoli, Italy

HIGHLIGHTS

- We have little knowledge on drought impacts on mixed Mediterranean forests.
- We analyzed Mediterranean mixed broadleaves forests affected by the 2017 drought.
- Most study stands showed a rapid growth recovery after drought.
- In some sites, stand structural overshoot predisposed to drought damage.
- Overshoot drought responses depend on historical pre-drought conditions.

GRAPHICAL ABSTRACT

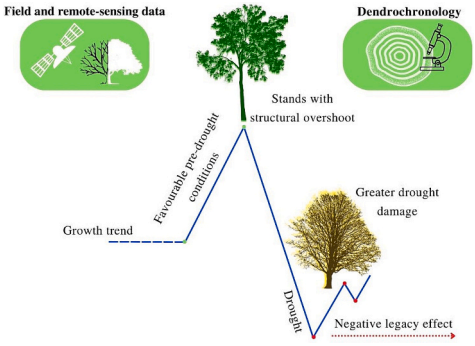

ARTICLE INFO

Editor: Manuel Esteban Lucas-Borja

Keywords:
Acer monspessulanum
Dendroecology
Drought overshoot
Fraxinus ornus
Legacy effects
Mediterranean forests
Resilience

ABSTRACT

Previous favorable climate conditions stimulate tree growth making some forests more vulnerable to hotter droughts. This so-called structural overshoot may contribute to forest dieback, but there is little evidence on its relative importance depending on site conditions and tree species because of limited field data. Here, we analyzed remote sensing (NDVI) and tree-ring width data to evaluate the impacts of the 2017 drought on canopy cover and growth in mixed Mediterranean forests (*Fraxinus ornus*, *Quercus pubescens*, *Acer monspessulanum*, *Pinus pinaster*) located in southern Italy. Legacy effects were assessed by calculating differences between observed and predicted basal area increment (BAI). Overall, the growth response of the study stands to the 2017 drought was contingent on site conditions and species characteristics. Most sites presented BAI and canopy cover reductions during the drought. Growth decline was followed by a quick recovery and positive legacy effects, particularly in the case of *F. ornus*. However, we found negative drought legacies in some species (e.g., *Q. pubescens*, *A. monspessulanum*) and sites. In those sites showing negative legacies, high growth rates prior to drought in response to previous wet winter-spring conditions may have predisposed trees to drought damage. Vice versa, the positive drought legacy found in some *F. ornus* site was linked to post-drought growth release due to *Q. pubescens* dieback and mortality. Therefore, we found evidences of structural drought overshoot, but it was restricted to

* Corresponding author.
E-mail addresses: santain.italiano@unibas.it (S.S.P. Italiano), jjcamarero@ipe.csic.es (J.J. Camarero), marcoborghetti@unibas.it (M. Borghetti), michele.colangelo@unibast.it (M. Colangelo), angelo.rita@unina.it (A. Rita), francesco.ripullone@unibas.it (F. Ripullone).

https://doi.org/10.1016/j.scitotenv.2024.172166
Received 13 October 2023; Received in revised form 9 March 2024; Accepted 31 March 2024
Available online 3 April 2024

specific sites and species. Our findings highlight the importance of considering site settings such as stand composition, pre-drought conditions and different tree species when studying structural overshoot. Droughts contribute to modify the composition and dynamics in mixed forests.

1. Introduction

Warmer temperatures are increasing evaporative demand leading to more severe droughts and forest dieback worldwide (Allen et al., 2015; Choat et al., 2018). Therefore, it is crucial to assess the vulnerability of trees to drought and their recovery capacity. A low resilience could jeopardize some tree populations if the frequency and severity of droughts and heatwaves increase (Schwalm et al., 2017). Post-drought recovery informs on how trees are impacted by stress and how they recover, i.e. on their resilience (Lloret et al., 2011; Guada et al., 2016; Ingrisch and Bahn, 2018). For instance, partial post-drought recovery can lead to legacy or carryover effects often characterized by incomplete return to prior growth rates (Anderegg et al., 2015; Kannenberg et al., 2020). Previous growth conditions can also influence drought legacies (Peltier and Ogle, 2019) and thus growth recovery after drought (Fritts, 1976; Ogle et al., 2015; Camarero et al., 2018; Pretzsch, 2021). For example, recurrent mild drought stress may improve drought resistance through physiological adjustments or metabolic changes (Backhaus et al., 2014). Thus, environmental events (dry and wet years) over time drive growth responses to drought (Serra-Maluquer et al., 2021). Further, the recovery of forests after water shortages and warm conditions can be influenced by both pre- and post-drought climatic conditions (Sergent et al., 2014).

Wet conditions after a drought can offset growth losses caused by previous dry conditions (Jiang et al., 2019), whereas favorable conditions that stimulate growth before a drought event could also predispose to dieback. In this context, a high aboveground biomass (high shoot-to-root ratio) due to favorable weather conditions, known as structural overshoot, may increase the risk of drought damage and exacerbate dieback (Jump et al., 2017). Temporal discrepancies between water availability and demand could potentially lead some stands to become overbuilt, leaving them susceptible to subsequent periods of dry and stressful conditions. However, there is still limited field evidence of the importance of structural overshoot as driver of drought responses in mixed forests with different site conditions and stand composition.

Considering also that species mixing and thus biodiversity can moderate the impact of disturbances (Lloret et al., 2007; Pretzsch et al., 2013; Bochenek et al., 2018), mixed forests may differently respond to drought as compared to pure stands (Camarero et al., 2021) by adopting different strategies. For example, the oak *Quercus pubescens* Willd. shows a high water use (anisohydric strategy) across its distribution area in central and southern Europe (Damesin and Rambal, 1995; Poyatos et al., 2008); thus, severe droughts may expose this species to hydraulic collapse. However, the ash *Fraxinus ornus* L., which coexists with *Q. pubescens* in southern Europe, seems to have a relatively low water use (isohydric strategy) with rapid post-drought recovery making it more tolerant to severe droughts (Tomasella et al., 2019). Both oak and ash form ring-porous wood. In contrast, Mediterranean pines such as *Pinus pinaster* Ait. show a strong regulation of leaf water potential regardless of environmental conditions and close their stomata during drought making them prone to drought-induced dieback (Ripullone et al., 2007; Valeriano et al., 2021). Lastly, we also considered a minor hardwood species forming diffuse-porous wood, *Acer monspessulanum* L., a Mediterranean maple species found from southern Europe to western Asia, which is considered drought-tolerant and resistant to xylem cavitation (Tissier et al., 2004), and shows a growth performance similar to oaks in seasonally dry sites (Portoghesi et al., 2008). There is still very little knowledge on the responses to drought of minor hardwood Mediterranean species, such as *F. ornus* and *A. monspessulanum*, despite their ecological and economic relevance. Both species provide resources such as wood and timber (Pignatti, 1982). The ash is also cultivated for the production of "manna", the crystallised sap in the shape of tear drop, that is widely used in the pharmaceutical and food industries (Caudullo and De Rigo, 2016). Further, the ability to resprout after cutting makes this ash species also well adapted to grow in areas disturbed by drought, wildfires and browsing. This species shows a high resistance to drought and it is often considered a suitable species for warmer and drier climate scenarios (Kowarik, 2023). However, we still lack data on the ash capacity to replace widely distributed species such as oak after severe droughts.

There is also little information on how site conditions can influence recovery in relation to factors such as soil depth and water retention capacity, slope, stand structure and composition, among others (Bréda et al., 2006; Ruehr et al., 2019). Indeed, different recovery rates among coexisting tree species or in sites with different quality affect post-disturbance forest resilience (Johnstone et al., 2016). Disturbances generate biological legacies that interact with soil properties such as water and nutrient availability (González de Andrés et al., 2022) and site-specific conditions mediate species responses to drought as has been shown in southern Europe (Rita et al., 2020). However, there is still a lack of information on recovery dynamics in different tree species under contrasting site conditions, considering pre- and post-drought conditions.

In this study we analyzed the recovery trajectories after the severe 2017 summer drought which strongly affected mixed Mediterranean forests in southern Italy (Italiano et al., 2023). We investigated six sites dominated by different tree species (*F. ornus*, *Q. pubescens*, *A. monspessulanum* and *P. pinaster*) showing differences in slope, aspect, elevation, soil and type of substrate (see also Coluzzi et al., 2020). This study was designed to identify differences in drought response among species co-occurring in mixed Mediterranean forests under contrasting site conditions. Achieving this aim is relevant to predict which species will better tolerate aridification and have better chance of establishing or replacing species with a low drought tolerance (cf. Batllori et al., 2020). Our specific objectives were to quantify the impacts of drought on canopy cover and radial growth rates using remote sensing (NDVI, Normalized Different Vegetation Index) and tree-ring data, respectively, to evaluate the radial growth responses to climate variables (temperature, precipitation and a drought index), and to quantify post-drought growth recovery and legacies. We hypothesize that high growth rates in trees before the drought, due to prior winter-spring wet conditions (i.e. structural overshoot), may increase vulnerability to drought damages and generate subsequent negative legacies linked to structural overshoot, particularly in sites with higher productivity.

In order to understand the phenomena that affected the study area before 2017, we also took into account two previous droughts which affected the forests of the study region (Basilicata, southern Italy) in 2003 and 2012 (Gentilesca et al., 2017; Colangelo et al., 2017, 2018). Furthermore, to characterize the status of the stands canopies with respect to the 2017 drought, we used NDVI series, as this index allows us to detect the loss of canopy and green cover (Coluzzi et al., 2020).

2. Materials and methods

2.1. Study sites

We selected six sites located in the Basilicata region (southern Italy, longitude 15.46–16.15° E, latitude 40.52–40.62° N), which were damaged by the 2017 severe summer drought (Fig. 1, Table 1). All selected sites are high, even-aged forests, except for the Palazzo site

(hereafter AP), where both high-forests and coppice are present. Here, former coppiced stands were converted to high-forests following the cessation of coppice management in recent decades. All the analyzed sites have experienced little or no management in the recent past.

Study sites were identified because they showed visual symptoms of dieback following the 2017 drought. Damage symptoms included premature leaf browning and shedding, canopy and shoot dieback and elevated tree mortality (see Italiano et al., 2023). Sites had different elevations (530–790 m a.s.l.), slopes (15–50 %), aspects (mainly N-NW but also S-SE at site Castelmezzano) and substrate or soil types (mainly sandstone but also limestone in Vietri di Potenza site and clay in Orto Siderio site, see Table 1).

Climate conditions in each study site were characterized using short-term records (period 2006–2020) from nearby meteorological stations (Table S1). In the study area, warmest and driest conditions occur in July and August and coldest conditions in January and February, while March and November are the wettest months.

The Accettura site (hereafter AP) has an average annual rainfall of 734 mm and a mean annual temperature of 16 °C. The forest consists of *Q. pubescens* mixed with *F. ornus* managed as coppice. The Grotta dell'Angelo site (hereafter GA) consists of broadleaves (*F. ornus*, *Carpinus orientalis* Mill, *Quercus ilex* L.) and conifer plantations (*P. pinaster*). The average annual rainfall is 889 mm and the mean annual temperature is 13.0 °C. The Ortosiderio site (hereafter OS) is dominated by *Q. pubescens*, *F. ornus*, *C. orientalis*, *Quercus cerris* L. and *Ostrya carpinifolia* Scop. It has climatic conditions similar to site GA. Moreover, *Q. pubescens* dieback was very evident in several patches in site OS (Coluzzi et al., 2020). The Vietri di Potenza site (hereafter VP) is dominated by *Q. pubescens* and other broadleaves (*A. monspessulanum*, *C. orientalis*, *Crataegus monogyna* Jacq.). The average annual rainfall is 943 mm and the average annual temperature is 14.5 °C. The Pietrapertosa site (hereafter PI) is dominated by *Q. pubescens*, *F. ornus*, *O. carpinifolia*, *C. orientalis* and *Pistacia terebinthus* L. The average annual rainfall is 671 mm and the average annual temperature is 12.7 °C. Lastly, the Castelmezzano site (hereafter CA) consists of *Q. pubescens*, *F. ornus*, *A. monspessulanum*, *Cornus mas* L. and *P. terebinthus*. Climate conditions are as at site PI (see Table 1).

2.2. Climate data, soil moisture and drought index

Long-term monthly or seasonal climate data (mean temperature, total precipitation) were obtained for the period 1950–2021 (Figs. S1 and S2). They corresponded to the 0.5°-gridded E-OBS ver. 22.0 climate dataset, which has been subjected to quality and homogeneity tests (Cornes et al., 2018). We selected this dataset because it provides long-term regional climate records, allowing us to perform climate-growth correlations analysis with respect to the time span (50–60 years), whereas local climate stations records are short (10–20 years) and often heterogeneous.

Changes in drought severity were evaluated by using the Standardized Precipitation Evapotranspiration Index (SPEI) which was downloaded from the Global Drought Monitor webpage (http://spei.csic.es/index.html) at 0.5° resolution. The SPEI is a multiscalar drought index that considers effects of temperature and evapotranspiration on water availability with negative and positive values corresponding to dry and wet conditions, respectively (Vicente-Serrano et al., 2010). We obtained 3-, 6- and 12-month long SPEI values to assess drought severity at different temporal resolutions (Fig. S3). Looking at the SPEI variability, it is possible to appreciate the three considered droughts (2003, 2012 and 2017) and the greater severity of the 2017 drought (Fig. S3).

Gridded (0.1° resolution), monthly soil moisture data at 0–10 cm depth were also obtained for the period 1992–2018 based on land surface model simulations with observations-based forcing (precipitation data) (Rodell et al., 2004). To better characterize the drought under study (2017), we also obtained daily data (period 2012–2020) of relative humidity from meteorological stations located near the study sites (Table S1, Fig. S4).

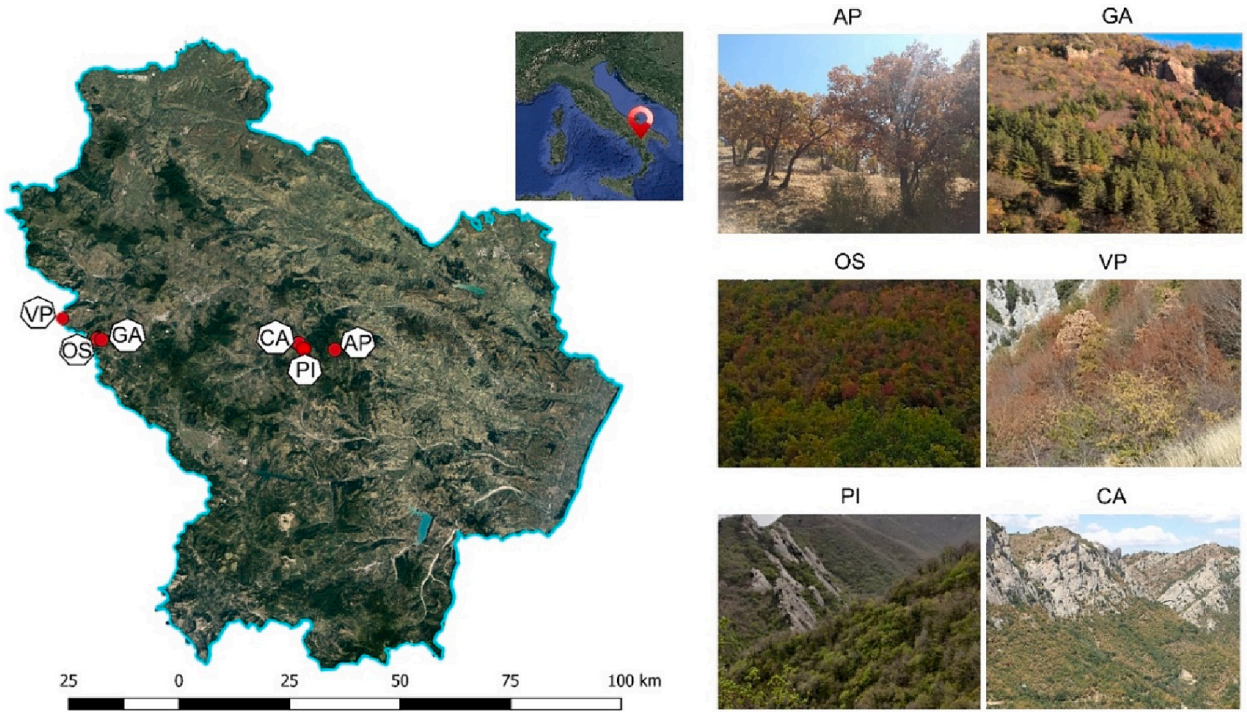

Fig. 1. Map showing the location of the six study sites in the Basilicata region (southern Italy) and images showing impacts of the 2017 summer drought (brown crowns, leaf shedding) in the six study sites. Site name abbreviations: AP, Accettura Palazzo; GA, Grotta dell'Angelo; OS, Ortosiderio; VP, Vietri di Potenza; PI, Pietrapertosa; CA, Castelmezzano.

2.3. Field sampling

At each site, an area of 5000 m^2 (circular in shape) was identified, representative of the entire stand in which we randomly sampled at least 15 dominant trees for each of the two most abundant species; thus, 30 trees per site, for a total of 180 trees were analyzed. The choice of selecting only dominant individuals instead of sampling all trees within the plot including sub-dominant individuals is justified because these latter being already weakened by the competition with dominant trees may be more sensitive to climatic stresses overestimating/underestimating drought impacts. Dominant trees are less affected by competition for light, nutrients and water than sub-dominant trees which are suppressed by their neighbors. For each tree, the diameter of the breast height (dbh) was measured twice in perpendicular at 1.3 m with a caliper, and the percentage of living or dead trees and the percentage of defoliation (crown transparency > 50 % or <50 %) in each representative area (5000 m^2) was also assessed (Dobbertin, 2005; Camarero et al., 2016) (Table 2).

2.4. Tree-ring data processing

Sampling was carried out, at the end of the 2021 growing season, by randomly selecting dominant trees. We took two cores from each tree at 1.3 m using a Pressler increment borer. Cores were dried and then smoothed with a slide microtome. In this way, the ring boundaries can be clearly distinguished (Gärtner and Nievergelt, 2010). All cores were visually cross-dated under a binocular microscope by assigning characteristic rings (Fritts, 1976). The ring widths were measured to the nearest 0.01 mm using the LINTAB 6-TSAPWin software (Rinntech, Heidelberg, Germany). The age at 1.3 m of each tree was estimated by counting the number of rings from bark to pith. Subsequently, the visual cross-dating of tree-ring series was checked by calculating moving correlations between the individual series and the mean series for each species at each site using the COFECHA software (Holmes, 1983), (see Table 3).

To assess the growth trend over time of the analyzed forest stands, we calculated the basal area increment (BAI) assuming a circular shape of stems. The individual ring-width series were transformed into BAI series corresponding to two-dimensional measures of stem area increment, which better reflects the growth of the entire tree than the one-dimensional series of tree-ring width. This was done using the formula:

$$BAI = \pi \left(R^2_t - R^2_{t-1}\right) \quad (1)$$

where R^2_t and R^2_{t-1} are the radii corresponding to the current (t) and prior (t-1) years, respectively.

To remove the BAI trends, the individual BAI series were detrended by fitting cubic smooth splines with a length of 67 % of the series using the ARSTAN software ver. 49 (Cook et al., 2017). Afterwards, an autoregressive model was applied to each detrended series to remove the first-order autocorrelation. This obtained residual or pre-whitened BAI series. Mean detrended BAI series were obtained by using bi-weight robust averages of detrended individual BAI series within each site and species ($n = 12$ series). These mean series or chronologies were used in further analyses considering the common, best-replicated 1980–2020 period. We used detrended BAI data for climate-growth relationships. Further, by detrending but keeping first-order autocorrelation the year-to-year drought impacts are highlighted. Legacy effects were assessed by subtracting observed from predicted BAI values calculated by removing the effects of post-drought climate conditions (Anderegg et al., 2015). In addition, the diameter annual increment was retrospectively calculated for each tree from ring-width measurements assuming non-eccentricity tree stems.

2.5. Characterizing impacts of drought using remote sensing data

We used the NDVI at a resolution of 10 m × 10 m to estimate canopy cover changes in each site and detect the impacts of the 2017 drought (Tucker and Sellers, 1986). The NDVI was obtained using Sentinel-2 products, already used to monitor the effects of drought on the studied stands (Coluzzi et al., 2020). The NDVI values were obtained from Google Earth Engine (https://developers.google.com/earth-engine/datasets/catalog/COPERNICUS_S2). The NDVI data were checked to exclude outliers (due to cloudiness). For each of the 6 analyzed stands, a polygon of 5000 m^2 was located in the middle of each stand to obtain mean monthly NDVI values during the growing season (April–September) and from 2016 to 2018. Finally, we calculated the ratios between the NDVI values measured in 2017 and 2016 ($NDVI_{2017}$/$NDVI_{2016}$) and between those measured in 2018 and 2017 ($NDVI_{2018}$/$NDVI_{2017}$) (see Table 1).

2.6. Correlations of growth indices with climate variables, soil moisture and the drought index

To evaluate growth responses to climate variability and drought severity we calculated Pearson correlation coefficients between detrended mean BAI series, monthly climate data (mean temperature and precipitation) and the SPEI (using 3-, 6- and 12-month temporal scales). Correlations were calculated from previous October to current September to account for lagged effects of prior climate conditions on tree growth. In the case of soil moisture, correlations were calculated for the same temporal window but considering the period 1992–2018. We considered the 0.05 and 0.01 significance levels in these analyses.

Climate, SPEI and humidity data have coarse spatial resolutions (0.1–0.5°), thereby precluding the possibility of making a detailed distinction of microclimatic conditions at each site. We are aware that different sites may exhibit varied elevation and exposure characteristics that could impact their respective microclimate conditions and drought impacts on trees. However, for the selected sites there are no other long-term climate data available that can provide information on a small scale, and the data from nearby weather stations do not have long and robust time series.

Table 1
Characteristics of the six sites studied in the Basilicata region, southern Italy. The temperature and precipitation values come from the records of the local meteorological stations (Table S1). MAT and TAP are the annual average and total annuals of temperature and precipitation, respectively, for each site.

Site	Longitude E (°)	Latitude N (°)	Elevation (m a.s.l.)	Slope (%)	Aspect	Substrate	MAT (°C)	TAP (mm)	Rainfall in 2017 compared to the average (%)
Accettura Palazzo (AP)	16.148	40.516	790	15	W	Sandstone	16	734	−25
Grotta dell'Angelo (GA)	15.558	40.570	760	30	N-NW	Clay	13	889	−29
Ortosiderio (OS)	15.546	40.573	600	35	N-NW	Clay	13	889	−29
Vietri di Potenza (VP)	15.460	40.617	530	30	NW	Limestone	14,5	943	−35
Pietrapertosa (PI)	16.058	40.533	625	35	N-NW	Sandstone	12,7	671	−18
Castellmezzano (CA)	16.054	40.534	665	50	S-SE	Sandstone	12,7	671	−18

Table 2
Characteristics of the six study sites, located in the Basilicata region, southern Italy. Stem diameter values (dbh) are means ± SD. The remote sensing indices are the ratio of the NDVI value pre and during the disturbance to the ratio post and during the disturbance. The first two letters represent the abbreviations of each site (AP, Accettura Palazzo; GA, Grotta dell'Angelo; OS, Ortosiderio; VP, Vietri di Potenza; PI, Pietrapertosa and CA, Castelmezzano); while the last two letters represent the abbreviations of the tree species analyzed at each site (FO, *Fraxinus ornus*; QP, *Quercus pubescens*; AM, *Acer monspessulanum* and PP, *Pinus pinaster*).

Code	Site	Sampled species	Species abundance (%)	Age (years)	Dbh (cm)	Dead trees (%)	Tres with severe crown defoliation (%)	$NDVI_{2017}$/ $NDVI_{2016}$	$NDVI_{2018}$/ $NDVI_{2017}$
APFO	AP	*Fraxinus ornus*	27.5	56	16.1 ± 3.8	0	0	1.178	0.887
APQP		*Quercus pubescens*	72.5	66	18.9 ± 6.6	0	45		
GAFO	GA	*Fraxinus ornus*	43.0	35	13.3 ± 3.2	0	0	1.064	0.940
GAPP		*Pinus pinaster*	57.0	33	33.1 ± 5.5	18	24		
OSFO	OS	*Fraxinus ornus*	44.0	42	9.0 ± 3.2	0	7	1.049	0.900
OSQP		*Quercus pubescens*	56.0	65	17.9 ± 6.8	61	89		
VPAM	VP	*Acer monspessulanum*	61.0	30	19.4 ± 5.8	0	64	0.939	1.116
VPQP		*Quercus pubescens*	39.0	45	22.2 ± 6.7	0	43		
PIFO	PI	*Fraxinus ornus*	19.0	58	7.1 ± 0.7	0	0	0.963	0.821
PIQP		*Quercus pubescens*	81.0	47	14.5 ± 5.1	11	45		
CAFO	CA	*Fraxinus ornus*	66.0	43	8.3 ± 2.4	3	10	0.897	0.943
CAQP		*Quercus pubescens*	34.0	50	16.2 ± 6.5	19	84		

Table 3
Growth data of the analyzed study sites located in the Basilicata region, southern Italy. Basal area increment (BAI) was calculated for the common period 1980–2020 (BAI values are means ± SE). Abbreviations: SD, standard deviation; AR1, first-order autocorrelation; MS, mean sensitivity. See sites' codes in Table 1.

Site	Species	Code	Interval	Tree-ring width (mm)	SD (mm)	AR1	MS	Correlation between growth series	BAI (cm^2 yr^{-1})
AP	FO	APFO	1938–2021	1.03	0.50	0.62	0.31	0.55	3.28 ± 0.11
	QP	APQP	1931–2021	1.14	0.63	0.72	0.26	0.66	4.22 ± 0.20
GA	FO	GAFO	1977–2021	1.65	0.66	0.61	0.29	0.57	3.71 ± 0.30
	PP	GAPP	1983–2021	3.11	1.80	0.83	0.23	0.68	23.68 ± 1.31
OS	FO	OSFO	1958–2021	0.76	0.40	0.61	0.31	0.48	1.20 ± 0.11
	QP	OSQP	1940–2021	1.20	0.57	0.71	0.22	0.53	5.84 ± 0.19
VP	AM	VPAM	1976–2021	2.19	0.83	0.46	0.33	0.54	7.60 ± 0.48
	QP	VPQP	1966–2021	1.90	1.00	0.66	0.32	0.71	8.18 ± 0.42
PI	FO	PIFO	1953–2021	0.82	0.48	0.66	0.33	0.58	1.35 ± 0.08
	QP	PIQP	1951–2021	1.07	0.80	0.73	0.36	0.65	2.90 ± 0.18
CA	FO	CAFO	1969–2021	0.93	0.45	0.61	0.30	0.55	1.95 ± 0.08
	QP	CAQP	1968–2021	1.50	1.13	0.86	0.27	0.63	5.47 ± 0.30

2.7. Growth resilience indices

To analyze post-drought growth recovery after selected dry years (2003, 2012 and 2017; see Fig. S3) we used the resilience indices proposed by Lloret et al. (2011): resistance (hereafter Rt), recovery (hereafter Rc), resilience (hereafter Rs), relative resilience (hereafter Rr) and impact (hereafter I). By considering mean BAI values before (PreDr), during (Dr) and after (PostDr) the drought, resilience indices were calculated as follows:

$$Rt = Dr/PreDr \quad (2)$$

$$Rc = PostDr/Dr \quad (3)$$

$$Rs = PostDr/PreDr \quad (4)$$

$$Rr = (PostDr - Dr)/PreDr \quad (5)$$

$$I = (PreDr - Dr)/PreDr \quad (6)$$

We chose three-year intervals to calculate these indices since legacy effects have been shown to be strong one-three years after drought (Anderegg et al., 2015). We also calculated resilience indices using one-year intervals and compared them with three-year indices (Schwarz et al., 2020). The resilience indices are defined as follows: Rt is the ability to resist growth reduction during the disturbance episode, i.e. the lower the value $Rt < 1$, the lower the resistance; Rc is the increase in growth compared to the minimum growth during the stress episode, $Rc < 1$ indicates growth decline and $Rc > 1$ indicates recovery; Rs is the ability to reach pre-episode growth levels; $Rs \geq 1$ indicates full recovery, whereas $Rs < 1$ indicates a decline in growth and low resilience; Rr is the resilience weighted by the damage suffered during the episode, and the closer this value is to 1 (0), the greater (lower) the relative resilience; finally, the closer the I value is to 1 the greater the impact suffered, while the closer the I value is to 0 the less impact suffered.

2.8. Statistical analyses

We used Mann-Kendall trend tests to assess if there were significant ($p < 0.05$) trends in climate data at seasonal resolution. Pearson and Spearman correlations were used to quantify relationships in the case of variables following or not following the normal distribution, respectively. Mann-Whitney tests were used to compare resilience indices

among sites, species and droughts.

We used linear mixed models (LMMs; Pinheiro and Bates, 2000) to model (log-transformed) BAI or resilience indices (Rt, Rc, Rs, Rr). BAI was modeled as a function of: species, tree dbh, calendar year, BAI of the previous year, drought severity (6-month SPEI); and tree was considered the random factor. The 2017 resilience indices were modeled as a function of: tree age and dbh, 2003 and 2012 resilience indices; in this case, the IDs of the trees of each species at each site were regarded as random factors.

We considered random effects in the models and quantified intra-class correlation coefficient (ICC) accounted by each factor, which allows assessing how much of the overall variation in the response variable is explained by grouping random effects, with higher values corresponding to greater between-group variability. Variances were estimated using restricted maximum likelihood (REML) methods. We also calculated the proportion of variance explained by fixed and by fixed plus random terms, which corresponded to the marginal (R^2m) and conditional R^2 (R^2c) values, respectively (Nakagawa et al., 2017). These

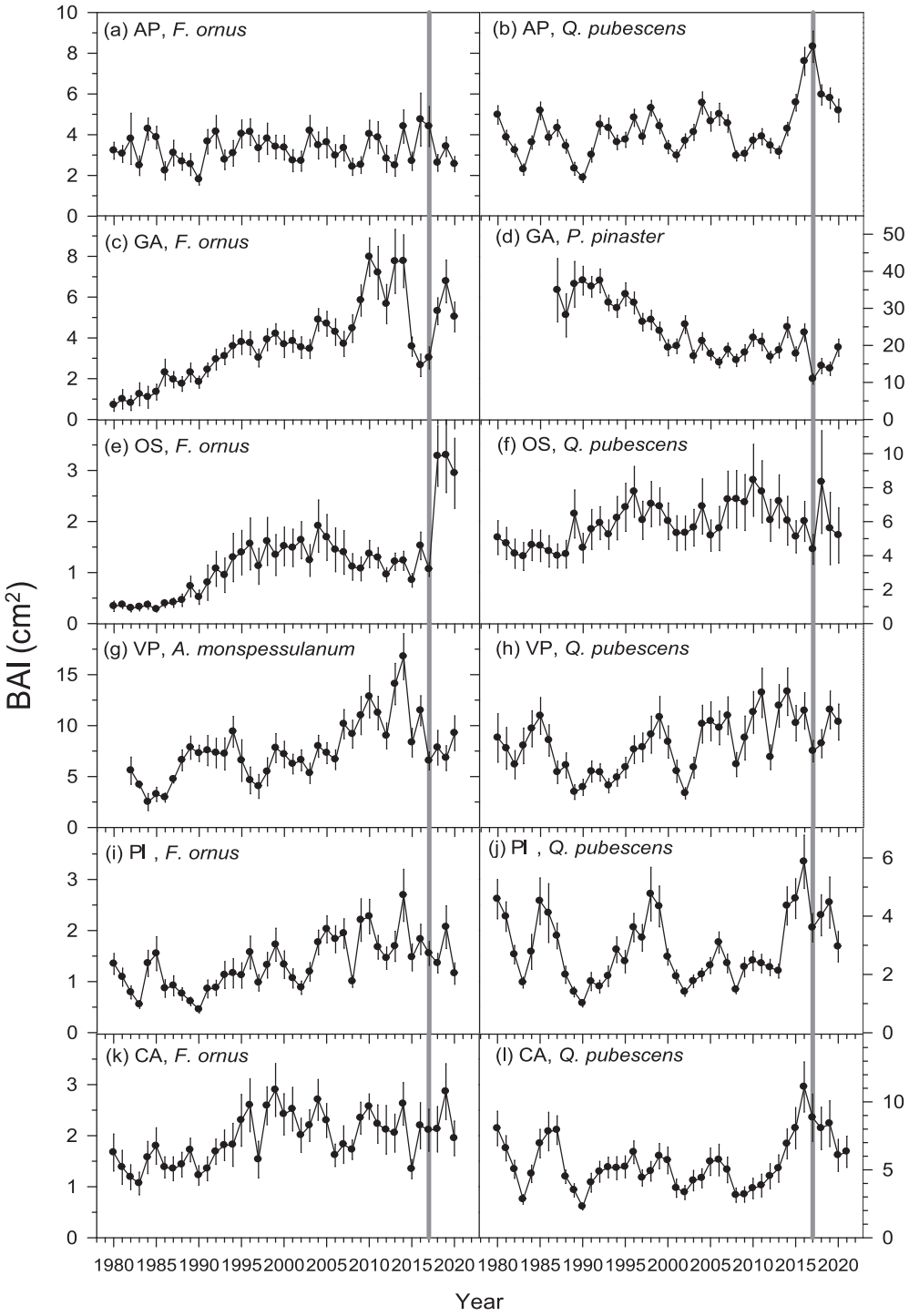

Fig. 2. Basal area increment (BAI) measured in the study sites (AP, Accettura Palazzo; GA, Grotta dell'Angelo; OS, Ortosiderio; VP, Vietri di Potenza; PI, Pietrapertosa and CA, Castelmezzano; located in the Basilicata region, southern Italy) for each species analyzed (values are means ± SE). The vertical grey lines indicate the 2017 drought.

were obtained using the r.squared GLMM function in the MuMIn package (Barton, 2022). Finally, a residual diagnosis was performed to check model assumptions, namely normality and homoscedasticity of residuals. LMMs' parameters were estimated using the lme4 R library (Bates et al., 2015). All statistical analyses were carried out with R (R Core Team, 2022).

3. Results

3.1. Climate trends and drought severity in 2017

Maximum and minimum temperatures, and also spring precipitation increased in the study area from 1950 to 2020 (Figs. S1 and S2). The SPEI values showed three major recent droughts occurring in 2003, 2012 and 2017, although drought severity peaked in 2017 (Fig. S3). The low relative air humidity values confirmed the elevated evaporative demand experienced by vegetation during 2012 and 2017 summers (Fig. S4). The 2017 drought was preceded by high winter-to-spring precipitation in the late 2000s and early 2010s.

3.2. Crown defoliation and growth patterns

Site crown defoliation varied from 0 to 90 % with OS and CA sites reaching the maximum defoliation percentages (Table 2). In almost all sites, *Q. pubescens* was the most affected species displaying the maximum defoliation values, while *F. ornus* showed lower values.

The tree-ring widths and BAI ranged 0.8–3.1 mm and 1.2–23.7 cm^2 yr^{-1}, respectively (Table 3). Minimum and maximum growth rates corresponded to *F. ornus* (site OS) and *P. pinaster* (site GA), respectively. *Q. pubescens* showed the highest first-order autocorrelation (site CA) and mean sensitivity (site PI) values, while *A. monspessulanum* presented the lowest autocorrelation (site VP). The mean correlation between the individual series and their corresponding mean site series ranged between 0.5 (site OS, *F. ornus*) and 0.7 (site VP, *Q. pubescens*) indicating a reliable cross-dating (Table 3).

Most sites presented a BAI reduction during the 2017 drought, but there were exceptions to this pattern such as *F. ornus* and *Q. pubescens* at site AP (Fig. 2). Here, both species showed a growth reduction in 2018. In the case of *F. ornus* at site GA, the 2017 growth drop was preceded by low BAI values in 2015 and 2016. Growth recovery after 2017 was evident in several sites such as GA, OS, VP, PI and CA, particularly in the case of *F. ornus*. A growth release was evident for *F. ornus* at site OS since BAI in the period 2018–2020 increased three times as compared with BAI in 2017. However, in the case of *Q. pubescens* from site CA growth declined after 2017. In general, growth reductions were also observed during the 2003 and 2012 droughts. In contrast, growth increases during the early 2010s occurred in some species and sites (*F. ornus* at site GA, *Q. pubescens* at site OS, *A. monspessulanum* at site VP).

3.3. Growth responses to climate variables

Warm and dry spring conditions were associated with lower growth rates of *F. ornus* (Fig. S10). However, there were exceptions with some sites where growth positively responded to wet prior-winter conditions (site PI) or cool current spring (site AP) conditions. The growth of *Q. pubescens* was favoured by wet and warm winter-spring conditions. However, in site OS, cold conditions during the previous autumn enhanced of *Q. pubescens*. In the case of *A. monspessulanum*, growth increased as rainfall increased from the previous winter to the current summer and also in response to low summer temperatures. A warmer winter and cool spring also favoured the growth of *P. pinaster*, which also benefited from late summer rains.

3.4. Growth responses to drought and soil moisture

Growth significantly increased as drought severity decreased in most sites and species, excepting *F. ornus* and *Q. pubescens* at site AP (Fig. 3). Another exception is *F. ornus* at the OS site, which showed a significant negative correlation from October to April with the 12-month SPEI.

The highest correlations were found from May to July considering 3-month SPEI values in the case of *A. monspessulanum*, *P. pinaster*, *F. ornus* at site OS (July only), and *F. ornus* and *Q. pubescens* (for oak only July) at site CA. However, more consistent growth-drought associations were found in the other sites showing responses to drought considering either 6- (*Q. pubescens* in OS site, *F. ornus* and *Q. pubescens* in PI site) or 12-month (*Q. pubescens* in VP site) SPEI values.

The highest correlations between growth and soil moisture were found in May and June (Fig. S11), and peaked in the case of *Q. pubescens* at sites VP and PI and *F. ornus* at site PI. The geographic influence of the relationships between growth and soil moisture in responsive species and sites (*Q. pubescens* at site VP) was broad, as showed the significant spatial correlations found across southern Italy (Fig. S5).

3.5. Growth and NDVI resilience indices

The resilience indices based on three-year periods (Fig. 4) were

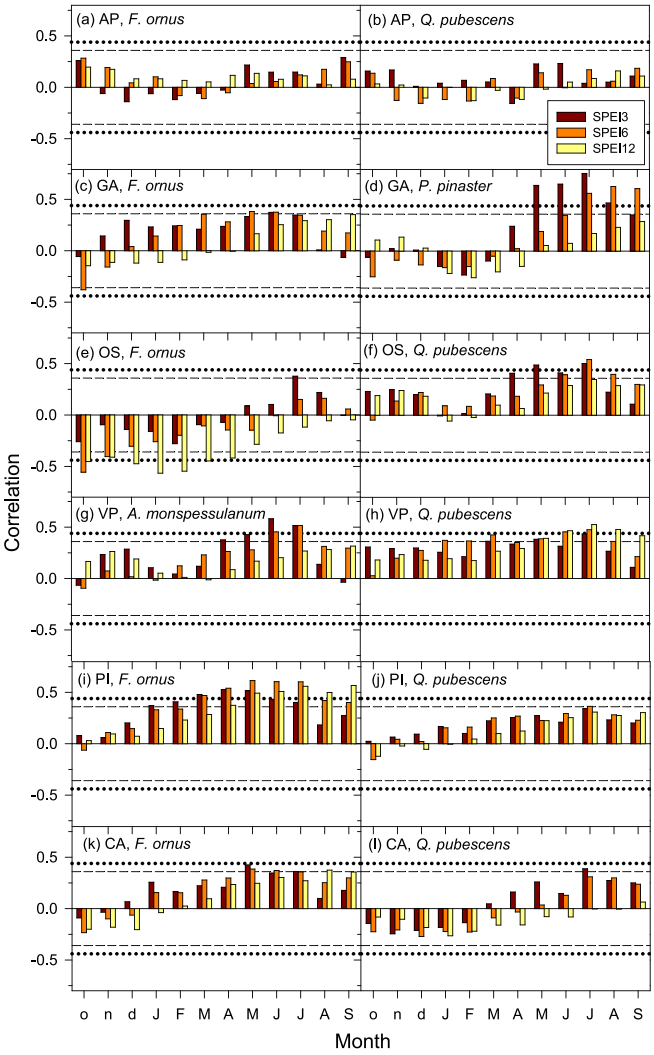

Fig. 3. Drought-growth relationships (Pearson coefficients) calculated for the study sites and species (located in the Basilicata region, southern Italy) considering 3- (SPEI3), 6- (SPEI6) and 12-month (SPEI12) long SPEI values. The window of analyses was from prior October to current September. Months of the previous year are abbreviated by lowercase letters. Dashed and dotted horizontal lines show the 0.05 and 0.01 significance levels, respectively.

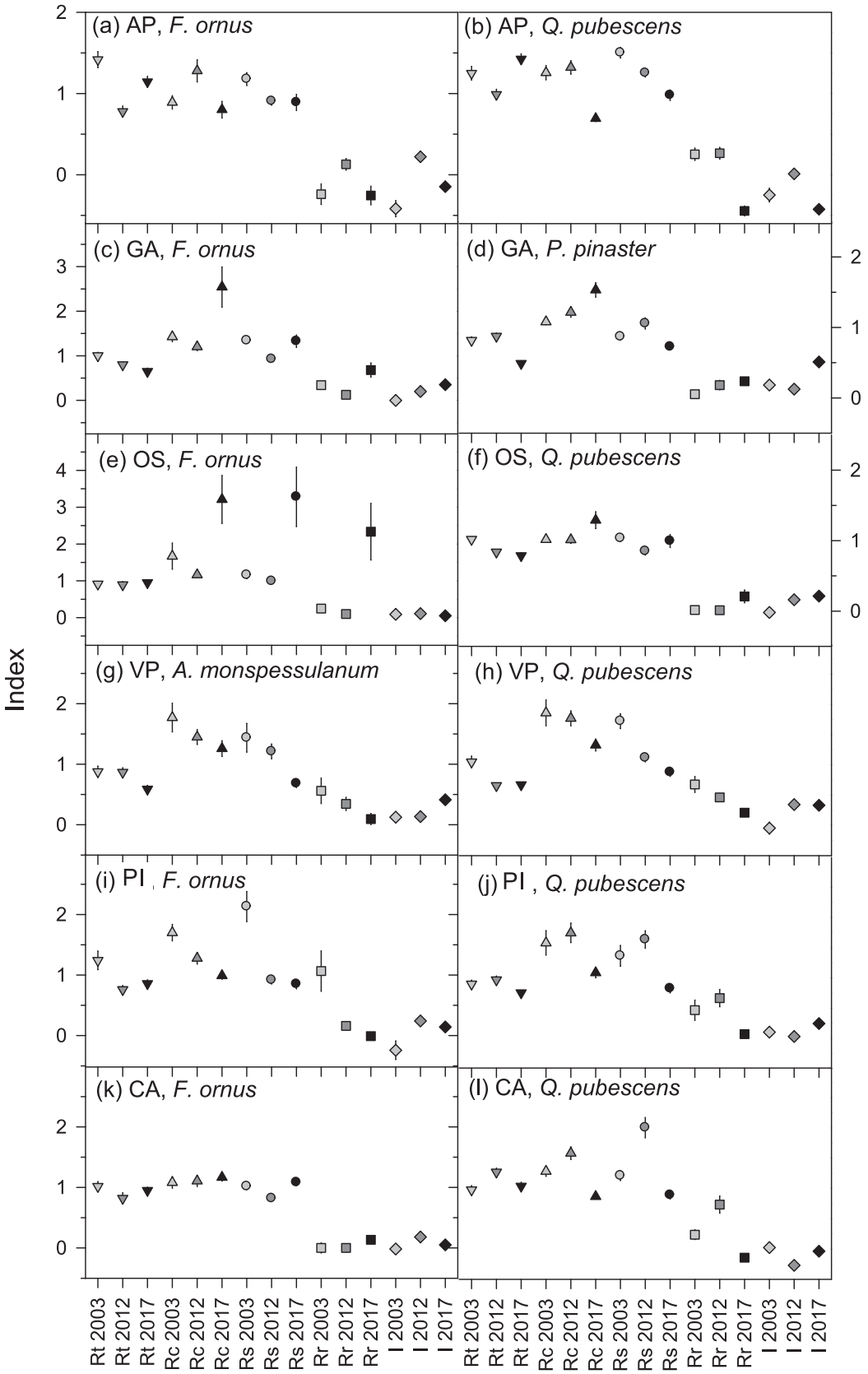

Fig. 4. Resilience indices, for each site and species analyzed (Basilicata region, southern Italy), obtained using basal area increment values for periods of 3-years before, during and 3-years after, each drought year considered (2003, 2012 and 2017). Values are means ± SE. The abbreviations of the resilience indices are: Rt, resilience (inverted triangles); Rc, recovery (triangles); Rs, resilience (dots); Rr, relative resilience (squares); I, impact (rhombuses). See the comparisons in Tables S2 and S3.

similar to those obtained based on one-year long periods (Fig. S6). Therefore, here we report results based on three-year periods. At sites GA and OS, and *F. ornus* presented very high recovery indices after the 2017 drought, followed by *P. pinaster* at site GA (Fig. 4, Table S2). Resistance after 2017 was lower than in the other two droughts. The post-2017 resilience was high in *F. ornus* from site OS illustrating the effect of the post-drought growth release (Figs. 2 and 4). However, the resilience and relative resilience after 2017 tended to be lower than after the 2003 and 2012 droughts, whereas the impact tended to increase.

Considering the comparisons of resilience indices among coexisting species, *Q. pubescens* showed higher resilience after 2017 than *F. ornus* at sites AP and VP, but lower recovery at sites OS and CA (Table S3). Relative resilience and impact were usually higher in *F. ornus*. Considering the NDVI responses to the 2017 drought, the lowest resistance values ($NDVI_{2017}/NDVI_{2016}$) were observed at sites CA, PI and VP, while the highest recovery values ($NDVI_{2018}/NDVI_{2017}$) were found at sites GA, VP and CA (Table 1).

3.6. Modeling post-drought recovery and legacies

Regarding the 2017 resilience indices, models were able to explain a low amount of variance as function of fixed factors, ranging between 2 % (recovery, relative resilience) and 8 % (resistance) (Table S4). Tree dbh was negatively associated to resistance after 2017, whereas the resilience in 2017 was negatively related to 2012 resilience (Fig. S7). Tree age at 1.3 m was negatively associated to the impacts after 2003 and 2017 droughts (Fig. S8). In contrast, BAI models resulted in robust fits (Fig. S9, Tables 4 and S5). BAI depended on prior growth, tree species and tree dbh. The fixed factors accounted for 12 % (site VP) to 42 % (site GA) of the total BAI variance, showing that random effects accounted for most growth variability.

Negative legacy effects lasting two years were found at sites VP (*Q. pubescens* and *A. monspessulanum*) and GA (only in *P. pinaster*) (Fig. 5). Positive and high BAI residuals during 2017, suggesting no negative impact of the 2017 drought on growth, were found for *F. ornus* at site AP and *Q. pubescens* at site CA. Lastly, slight positive legacy effects were observed in the case of *F. ornus* at sites OS and AP, and *Q. pubescens* at sites PI and CA. In addition, GA and VP sites exhibited negative drought legacies (Fig. 5). These effects were stronger at site VP, particularly in the case of *A. monspessulanum*, which also showed higher crown defoliation than *Q. pubescens* (Table 2). In site GA, a negative legacy was found for *P. pinaster*, which showed higher crown defoliation (24 %) than the co-occurring *F. ornus* (0 %).

4. Discussion

4.1. Responses to drought: structural overshoot and legacy effects

In general, consistent negative growth responses to drought were found when considering mid or long-term droughts (6- to 12-month SPEI values) for most sites and species. The highest correlations between growth and soil moisture were found in late spring and early summer, peaking in the case of *Q. pubescens* and *F. ornus* at site PI.

In most study sites and species, the 2017 drought was followed by a fast recovery and positive legacy effects. This finding confirms the Mediterranean forests tendency to recover after extreme drought events and is consistent with previous studies (Gazol et al., 2018).

We also contributed to explain forest vulnerability to drought by considering structural overshoot, which may be a key characteristic of productive mixed Mediterranean forests subjected to a high year-to-year precipitation variability. We found support for our hypothesis of a significant legacy effect in the extreme 2017 drought that mainly affected two sites (GA and VP) and, in particular, *P. pinaster* and *A. monspessulanum*. The lack of shared legacy effects during the 2017 drought could be attributed to variations in drought tolerance among coexisting tree species. Certainly, being *P. pinaster* a planted and non-native species it could be more negatively affected by drought than native species such as *F. ornus* (Camarero et al., 2021). Furthermore, *P. pinaster* roots show a decrease in the concentration of non-structural carbohydrates under drought, indicating the depletion of carbon pools (Jacquet et al., 2014).

Fraxinus ornus showed a remarkable recovery not only in comparison to *P. pinaster*, but also compared to *Q. pubescens*. This ash species also showed the lowest crown defoliation (ranging 0–10 %), further

Table 4
Summary statistics (factor; SE, standard error) of linear mixed models fitted to basal area increment (BAI) measured in the six study sites (Basilicata region, southern Italy). Models were fitted as a function of tree species (Spp), calendar year, BAI of the previous year (BAI_{t-1}), diameter at breast height (dbh), and 6-month SPEI (spei6). Species' abbreviations: QP, *Quercus pubescens*; FO, *Fraxinus ornus*; PP, *Pinus pinaster*; AM, *Acer monspessulanum*. Tree ID is the random term. The last line shows the proportion of variance explained by fixed (R^2m) and by fixed plus random terms (R^2c). Significance levels: *p < 0.05, **p < 0.01, ***p < 0.001.

Variables	Study sites											
	Accettura Palazzo (AP)		Grotta dell'Angelo (GA)		Ortosiderio (OS)		Vietri di Potenza (VP)		Pietrapertosa (PI)		Castelmezzano (CM)	
	Factor	SE	Factor	SE	Factor	SE	Factor	SE	Factor	SE	Factor	SE
Intercept	0.34	0.28	1.00 ***	0.22	2.83 ***	0.51	0.28	0.19	0.70	0.37	1.08 **	0.34
Spp [QP]	−0.78	0.42			−3.14 ***	0.73	0.39 ***	0.03	−1.11 *	0.54	−1.97 ***	0.51
Year	−0.23 ***	0.05	−0.34 ***	0.05	−0.32 ***	0.05	−0.16 **	0.05	0.40 ***	0.03	−0.44 ***	0.06
BAI_{t-1}	0.36 ***	0.03	0.39 ***	0.03	0.33 ***	0.03	−0.32	0.27	−0.21 ***	0.05	0.38 ***	0.03
Spp [FO] * dbh	0.77 ***	0.22	1.63 ***	0.25	3.46 ***	0.63			1.05 **	0.38	1.53 ***	0.40
Spp [QP] * dbh	1.15 ***	0.22			1.51 *	0.60	0.69 **	0.26	1.43 ***	0.37	2.05 ***	0.40
Spp [FO] * spei6	0.02	0.02	0.05 **	0.02	0.02	0.01			0.05 *	0.03	0.03	0.02
Spp [QP] * spei6	0.03	0.02			0.04 **	0.01	0.06 **	0.02	0.09 ***	0.02	0.07 ***	0.02
Spp [PP]			−0.77 *	0.33								
Spp [PP] * dbh			0.56 **	0.20								
Spp [PP] * spei6			0.07 ***	0.02								
Spp [AM] * dbh							0.51 *	0.24				
Spp [AM] * spei6							0.10 ***	0.03				
Random effects												
σ^2	0.09		0.10		0.10		0.14		0.15		0.11	
τ_{00}	2.20_{Tree}		1.15_{Tree}		5.70_{Tree}		2.11_{Tree}		2.22_{Tree}		3.68_{Tree}	
τ_{11}	$0.01_{Tree.dbh}$		$0.00_{Tree.dbh}$		$0.09_{Tree.dbh}$		$0.01_{Tree.dbh}$		$0.03_{Tree.dbh}$		$0.03_{Tree.dbh}$	
ρ_{01}	-0.92_{Tree}		-0.89_{Tree}		-0.85_{Tree}		-0.94_{Tree}		-0.87_{Tree}		-0.93_{Tree}	
ICC	0.96		0.92		0.98		0.94		0.94		0.97	
Observations	869		820		843		780		835		867	
R^2m/R^2c	0.14/0.96		0.42/0.95		0.28/0.98		0.12/0.94		0.23/0.95		0.24/0.97	

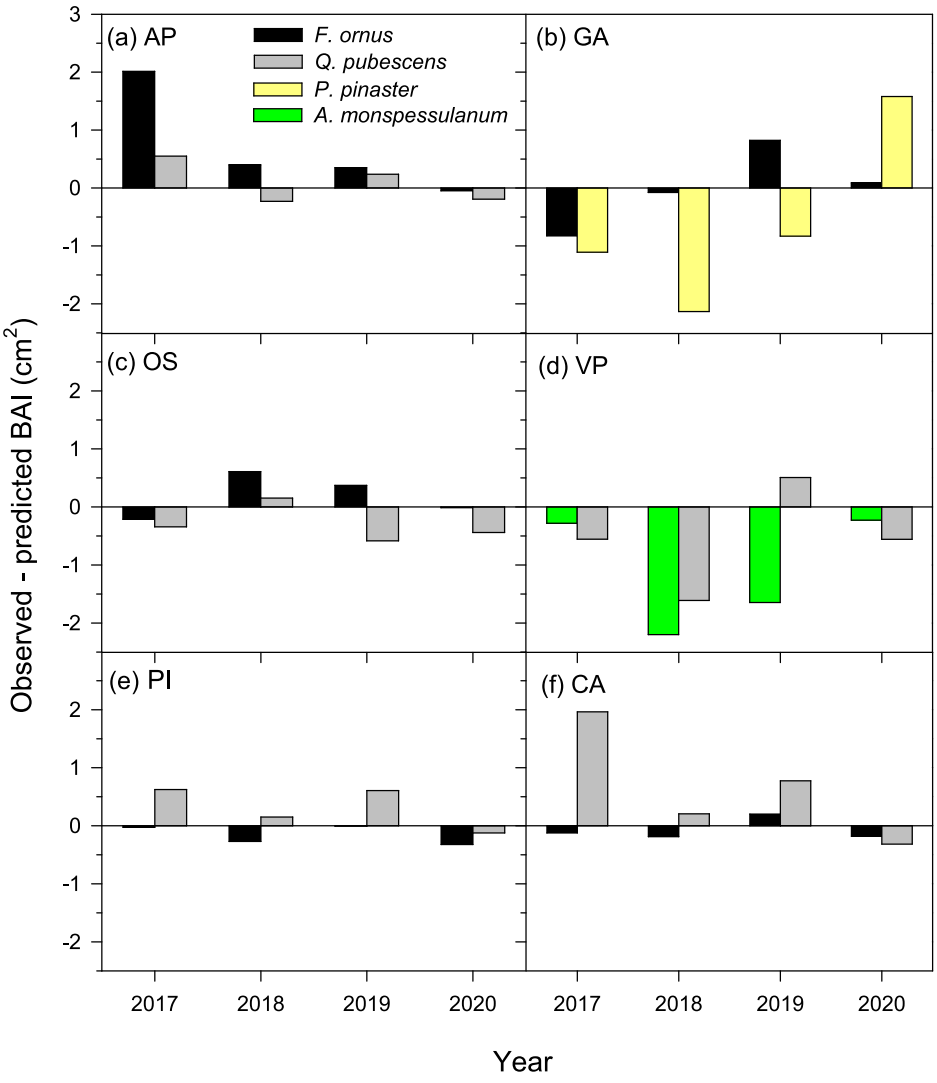

Fig. 5. Difference between observed and predicted BAI (cm^2), from the year 2017 to the year 2020, to show the legacy effects of the 2017 drought, for the four study species (FO, *Fraxinus ornus*; QP, *Quercus pubescens*; AM, *Acer monspessulanum* and PP, *Pinus pinaster*) and for each of the six sites analyzed (AP, Accettura Palazzo; GA, Grotta dell'Angelo; OS, Ortosiderio; VP, Vietri di Potenza; PI, Pietrapertosa and CA, Castelmezzano) in the Basilicata Region, Southern Italy.

confirming its resistance to drought. In addition, *F. ornus* is a species that shows good control of reserves for rapid post-drought recovery (Tomasella et al., 2019), and it allocates relatively more carbon to leaf biomass and conductive phloem under water shortage conditions (Kiorapostolou et al., 2019). These traits can provide this species a high post-drought resilience.

In the second site where more negative drought legacies were observed (site VP), the two coexisting species (*A. monspessulanum*, *Q. pubescens*) are drought-tolerant, so in terms of resilience indices they behaved similarly. However, *A. monspessulanum* was more affected by the drought, bringing with it negative legacies in the two years following the drought (see Fig. 5), compared to the anisohydric *Q. pubescens* (Damesin and Rambal, 1995; Poyatos et al., 2008), which probably gave it a small extra advantage with negative legacies evident only in the year following 2017. Globally, oaks exhibit a fast post-drought recovery (Anderegg et al., 2015), which could be explained by their ability to compensate for the loss of hydraulic conductivity by forming new earlywood, wide vessels (Cavender-Bares and Holbrook, 2001).

The fact that drought legacies were observed in planted (*P. pinaster*) and natural (*A. monspessulanum*) stands suggests that their different structure did not explain their responses to drought, but this should be validated by comparing different stand structures of each species. Overall, the GA and VP sites illustrate how the structural overshoot amplified drought damage after 2017 and contributed to negative legacies, as trees showed high pre-drought growth rates in response to wet winter-spring conditions. Thus, the damage was conditioned by previous moisture conditions that led to overbuilt stands. Our findings may be very important given how widespread forest dieback phenomena are (Allen et al., 2015). For instance, a recent global study estimated that structural overshoot contributed to exacerbate negative impacts in about 11 % of drought events in the period 1981–2015 (Zhang et al., 2021). Further research should also consider how forest composition and structure determine structural overshoot and post-drought legacies (Yu et al., 2022). We are aware that the legacy effects of the 2017 drought, calculated as differences between observed and predicted basal area increment (BAI), may be partially influenced by the low explained variance from some models for certain study sites, which could affect the predicted values of BAI.

However, we cannot exclude that impacts observed in response to the 2017 droughts were caused by other drivers not included in our analyses (i.e., stand basal area and density, competition, aboveground biomass, etc.). Even if this is the case, the choice of sampling only dominant individuals probably reduced likely risks due to competition that are more relevant in sub-dominant and suppressed trees, which may

overestimate/underestimate the drought impact. In fact, drought effects can be linked to whole stand water usage and not only to individual tree overshoot. Furthermore, mixed stands have greater resistance and resilience to drought events than pure stands, but the beneficial effect of species mixing cannot be generalized because it is strongly modulated by the type of mixing and the identity of the tree species (Pardos et al., 2021). Our findings also show that the characteristics of the site must also be considered when assessing drought resilience.

4.2. Site characteristics and species features

The negative growth responses to the 2017 drought were contingent on site conditions (slope, soil, exposure) and species characteristics. For instance, the *F. ornus* growth release observed in the OS site may be explained by the elevated *Q. pubescens* dieback (Table 2), which could have reduced competition for soil water and nutrients favouring *F. ornus*. A long-term legacy with a slow recovery in *Q. pubescens* compared to *F. ornus* could be also due to differences in structural damage after drought constraining the regrowth of damaged tissues (Gessler et al., 2020). Such repair and regrowth of lost or damaged tissues can exacerbate the depletion of non-structural carbon (Ouyang et al., 2021). In some study stands (e.g., the OS site), a progressive replacement of *Q. pubescens* by *F. ornus* could occur if more severe droughts occur. Indeed, increasing aridity is accelerating the shift of forest composition towards communities dominated by drought resistant species at a global scale (Batllori et al., 2020). In contrast, the increase in growth observed in *Q. pubescens* at some sites such as AP could be explained by the formation of most of the growth ring before the onset of summer drought. The different timing of radial growth and drought influences growth recovery (Camarero et al., 2015; Huang et al., 2018; van Kampen et al., 2022). In addition, *Q. pubescens* could have relied on non-structural carbohydrates stored in previous years to form the 2017 growth ring (Colangelo et al., 2017). This could explain why *Q. pubescens* showed a greater resistance than *F. ornus* to the 2017 drought. Moreover, AP is the warmest site where trees may be already adapted to cope with heat stress. For example, recent studies have observed that drought resilience has mainly increased in dry and warm sites (Pardos et al., 2021). The differences in resilience between coexisting species could be due to their different soil water uptake strategies which affect gas-water exchange dynamics (Lemoine et al., 2001), but this could be refined using soil and plant water isotopes and studies on root architecture (Yin et al., 2024). Lastly, future studies could consider tree-to-tree competition and compare growth data from dominant and suppressed trees to support our findings. Nevertheless, recent meta-analyses indicate that competition does not drive resilience to growth after drought in many cases (Castagneri et al., 2022).

5. Conclusions

Growth resilience and drought legacies depended on site and species characteristics. Most sampled sites showed a growth reduction during the 2017 drought. This growth reduction was followed by a quick recovery and positive legacy effects, which may be a feature characteristic of mixed, productive Mediterranean forests. Negative drought legacies, lasting up to two years, were mainly found in sites with low productivity and more unfavorable climate conditions. In these sites, trees showed high growth rates prior to drought in response to previous favorable winter-spring wet conditions which predisposed to drought damage and partially explained negative legacies.

We also present tree-ring data on understudied minor Mediterranean tree species (*F. ornus*, *A. monspessulanum*) which could represent alternative to more widely distributed species such as oaks (*Q. pubescens*) under warmer and drier climate conditions. During the 2017 drought, *Q. pubescens* exhibited greater resistance than *F. ornus*, but *F. ornus* showed a better recovery and *A. monspessulanum* exhibited significant resistance. All broadleaf trees studied showed a higher tolerance to drought than the planted pine (*P. pinaster*), indicating their higher performance than the introduced conifer under more arid conditions. Overall, *F. ornus* seems to be the species that responded best to drought in terms of growth recovery.

This study represents an important step in delineating the conditions for observing structural overshoot in mixed Mediterranean forests subjected to seasonal drought. Our results anticipate changes in stand composition towards communities dominated by more drought-tolerant tree species. Certainly, additional variables reflecting drought impacts on tree functioning such as wood anatomy, non-structural carbohydrate concentrations, soil water, nutrient availability and uptake would further strengthen the general overview on post-drought stand dynamics.

CRediT authorship contribution statement

Santain S.P. Italiano: Writing – review & editing, Writing – original draft, Methodology, Investigation, Formal analysis, Data curation, Conceptualization. **J. Julio Camarero:** Writing – review & editing, Writing – original draft, Visualization, Supervision, Funding acquisition, Formal analysis, Data curation. **Marco Borghetti:** Writing – review & editing, Visualization, Supervision, Funding acquisition. **Michele Colangelo:** Writing – review & editing, Methodology. **Angelo Rita:** Writing – review & editing, Validation, Formal analysis. **Francesco Ripullone:** Writing – review & editing, Visualization, Supervision, Methodology, Investigation, Funding acquisition, Conceptualization.

Declaration of competing interest

The authors declare that they have no known competing financial interests or personal relationships that could have appeared to influence the work reported in this paper.

Data availability

Data will be made available on request.

Acknowledgments

The Italian Ministry of University has supported this research in the framework of the project ARS01_00405, “OT4CLIMA, Advanced EO technologies for studying Climate Change impacts on the environment” (D.D. 2261 del 6.9.2018, PON R & I 2014-2020 and FSC). This study was also supported within the Agritech National Research Center and partially financed by the European Union Next-Generation funds (Piano Nazionale di Ripresa e Resilienza (PNRR) – Missione 4 Componente 2, Investimento 1. 4 – D.D. 1032 dopo17/06/2022CN00000022). JJC acknowledges support of the project CGL2015-69186-C2-1-R (Spanish Ministry of Science). We acknowledge the E-OBS dataset from the EU-FP6 project UERRA (http://www.uerra.eu) and the Copernicus Climate Change Service, and the data providers in the ECA&D project (https://www.ecad.eu).

Appendix A. Supplementary data

Supplementary data to this article can be found online at https://doi.org/10.1016/j.scitotenv.2024.172166.

References

Allen, C.D., Breshears, D.D., McDowell, N.G., 2015. On underestimation of global vulnerability to tree mortality and forest die off from hotter drought in the Anthropocene. Ecosphere 6, 1–55. https://doi.org/10.1890/ES15-00203.1.

Anderegg, W.R., Schwalm, C., Biondi, F., Camarero, J.J., Koch, G., Litvak, M., et al., 2015. Pervasive drought legacies in forest ecosystems and their implications for carbon cycle models. Science 349, 528–532. https://doi.org/10.1126/science.aab1833.

Backhaus, S., Kreyling, J., Grant, K., Beierkuhnlein, C., Walter, J., Jentsch, A., 2014. Recurrent mild drought events increase resistance toward extreme drought stress. Ecosystems 17, 1068–1081. https://doi.org/10.1007/s10021-014-9781-5.
Barton, K., 2022. MuMIn: Multi-Model Inference. Available online: https://cran.r-project.org/web/packages/MuMIn/index.html (accessed on 22 July 2022).
Bates, D., Mächler, M., Bolker, B., Walker, S., 2015. Fitting linear mixed-effects models using lme4. J. Stat. Soft. 67, 1–48. https://doi.org/10.48550/arXiv.1406.5823.
Batllori, E., Lloret, F., Aakala, T., Anderegg, W.R.L., Aynekulu, E., et al., 2020. Forest and woodland replacement patterns following drought-related mortality. Proc. Natl. Acad. Sci. U. S. A. 117, 29720–29729. https://doi.org/10.1073/pnas.2002314117.
Bochenek, Z., Ziolkowski, D., Bartold, M., Orlowska, K., Ochtyra, A., 2018. Monitoring forest biodiversity and the impact of climate on forest environment using high-resolution satellite images. Eur. J. Rem. Sens. 51, 166–181. https://doi.org/10.1080/22797254.2017.1414573.
Bréda, N., Huc, R., Granier, A., Dreyer, E., 2006. Temperate forest trees and stands under severe drought: a review of ecophysiological responses, adaptation processes and long-term consequences. Ann. For. Sci. 63, 625–644. https://doi.org/10.1051/forest:2006042.
Camarero, J.J., Franquesa, M., Sangüesa-Barreda, G., 2015. Timing of drought triggers distinct growth responses in holm oak: implications to predict warming-induced forest defoliation and growth decline. Forests 6, 1576–1597. https://doi.org/10.3390/f6051576.
Camarero, J.J., Sangüesa-Barreda, G., Vergarechea, M., 2016. Prior height, growth, and wood anatomy differently predispose to drought-induced dieback in two Mediterranean oak species. Ann. For. Sci. 73, 341–351. https://doi.org/10.1007/s13595-015-0523-4.
Camarero, J.J., Gazol, A., Sangüesa-Barreda, G., Cantero, A., Sánchez-Salguero, R., Sánchez-Miranda, A., Granda, E., Serra-Maluquer, X., Ibañez, R., 2018. Forest growth responses to drought at short- and long-term scales in Spain: squeezing the stress memory from tree rings. Front. Ecol. Evol. 6, 9. https://doi.org/10.3389/fevo.2018.00009.
Camarero, J.J., Gazol, A., Linares, J.C., Fajardo, A., Colangelo, M., Valeriano, C., Sánchez-Salguero, R., Sangüesa-Barreda, G., Granda, E., Gimeno, T.E., 2021. Differences in temperature sensitivity and drought recovery between natural stands and plantations of conifers are species-specific. Sci. Total Environ. 796, 148930 https://doi.org/10.1016/j.scitotenv.2021.148930.
Castagneri, D., Vacchiano, G., Hacket-Pain, A., DeRose, R.J., Klein, T., Bottero, A., 2022. Meta-analysis reveals different competition effects on tree growth resistance and resilience to drought. Ecosystems 25, 30–43. https://doi.org/10.1007/s10021-021-00638-4.
Caudullo, G., De Rigo, D., 2016. *Fraxinus ornus* in Europe: distribution, habitat, usage and threats. In: The European Atlas of Forest Tree Species: Modelling, Data and Information on Forest Tree Species. Publ. Off. EU, Luxembourg, pp. 100–101.
Cavender-Bares, J., Holbrook, N.M., 2001. Hydraulic properties and freezing-induced cavitation in sympatric evergreen and deciduous oaks with contrasting habitats. Plant Cell Environ. 24, 1243–1256. https://doi.org/10.1046/j.1365-3040.2001.00797.x.
Choat, B., Brodribb, T.J., Brodersen, C.R., Duursma, R.A., López, R., Medlyn, B.E., 2018. Triggers of tree mortality under drought. Nature 558, 531–539. https://doi.org/10.1038/s41586-018-0240-x.
Colangelo, M., Camarero, J.J., Battipaglia, G., Borghetti, M., De Micco, V., Gentilesca, T., Ripullone, F., 2017. A multi-proxy assessment of dieback causes in a Mediterranean oak species. Tree Physiol. 37, 617–631. https://doi.org/10.1093/treephys/tpx002.
Colangelo, M., Camarero, J.J., Borghetti, M., Gentilesca, T., Oliva, J., Redondo, M.A., Ripullone, F., 2018. Drought and *Phytophthora* are associated with the decline of oak species in southern Italy. Front. Plant Sci. 9 https://doi.org/10.3389/fpls.2018.01595.
Coluzzi, R., Fascetti, S., Imbrenda, V., Italiano, S.S.P., Ripullone, F., Lanfredi, M., 2020. Exploring the use of Sentinel-2 data to monitor heterogeneous effects of contextual drought and heatwaves on Mediterranean forests. Land 9, 325. https://doi.org/10.3390/land9090325.
Cook, E.R., Krusic, P.J., Peters, K., Holmes, R.L., 2017. Program ARSTAN (version 49), Autoregressive tree–ring standardization program. In: Tree–Ring Laboratory of Lamont–Doherty Earth Observatory. Columbia University, USA.
Cornes, R., van der Schrier, G., van den Besselaar, E.J.M., Jones, P.D., 2018. An ensemble version of the E-OBS temperature and precipitation datasets. J. Geophys. Res. Atmos. 123, 9391–9409.
Damesin, C., Rambal, S., 1995. Field study of leaf photosynthetic performance by a Mediterranean deciduous oak tree (*Quercus pubescens*) during a severe summer drought. New Phytol. 131, 159–167. https://doi.org/10.1111/j.1469-8137.1995.tb05717.x.
Dobbertin, M., 2005. Tree growth as indicator of tree vitality and of tree reaction to environmental stress: a review. Eur. J. For. Res. 124, 319–333. https://doi.org/10.1007/s10342-005-0085-3.
Fritts, H.C., 1976. Tree Rings and Climate. Academic Press, London.
Gärtner, H., Nievergelt, D., 2010. The core-microtome: a new tool for surface preparation on cores and time series analysis of varying cell parameters. Dendrochronologia 28, 85–92. https://doi.org/10.1016/j.dendro.2009.09.002.
Gazol, A., Camarero, J.J., Vicente-Serrano, S.M., Sánchez-Salguero, R., et al., 2018. Forest resilience to drought varies across biomes. Glob. Change Biol. 24, 2143–2158. https://doi.org/10.1111/gcb.14082.
Gentilesca, T., Camarero, J.J., Colangelo, M., Nolè, A., Ripullone, F., 2017. Drought-induced oak decline in the western Mediterranean region: an overview on current evidences, mechanisms and management options to improve forest resilience. iForest Biogeosci. For. 10, 796. https://doi.org/10.3832/ifor2317-010.
Gessler, A., Bottero, A., Marshall, J., Arend, M., 2020. The way back: recovery of trees from drought and its implication for acclimation. New Phytol. 228, 1704–1709. https://doi.org/10.1111/nph.16703.
González de Andrés, E., Gazol, A., Querejeta, J.I., Igual, J.M., Colangelo, M., Sánchez-Salguero, R., Camarero, J.J., 2022. The role of nutritional impairment in carbon-water balance of silver fir drought-induced dieback. Glob. Change Biol. 28, 4439–4458. https://doi.org/10.1111/gcb.16170.
Guada, G., Camarero, J.J., Sanchez-Salguero, R., Cerrillo, R.M.N., 2016. Limited growth recovery after drought-induced forest dieback in very defoliated trees of two pine species. Front. Plant Sci. 7, 418. https://doi.org/10.3389/fpls.2016.00418.
Holmes, R.L., 1983. Computer-assisted quality control in tree-ring dating and measurement. Tree-Ring Bull. 43, 68–78.
Huang, M., Wang, X., Keenan, T.F., Piao, S., 2018. Drought timing influences the legacy of tree growth recovery. Glob. Change Biol. 24, 3546–3559. https://doi.org/10.1111/gcb.14294.
Ingrisch, J., Bahn, M., 2018. Towards a comparable quantification of resilience. TREE 33, 251–259. https://doi.org/10.1016/j.tree.2018.01.013.
Italiano, S.S., Camarero, J.J., Borghetti, M., Colangelo, M., Pizarro, M., Ripullone, F., 2023. Radial growth, wood anatomical traits and remote sensing indexes reflect different impacts of drought on Mediterranean forests. For. Ecol. Manage. 548, 121406 https://doi.org/10.1016/j.foreco.2023.121406.
Jacquet, J.S., Bosc, A., O'Grady, A., Jactel, H., 2014. Combined effects of defoliation and water stress on pine growth and non-structural carbohydrates. Tree Physiol. 34, 367–376. https://doi.org/10.1093/treephys/tpu018.
Jiang, P., Liu, H., Piao, S., Ciais, P., Wu, X., Yin, Y., Wang, H., 2019. Enhanced growth after extreme wetness compensates for post-drought carbon loss in dry forests. Nat. Commun. 10, 195. https://doi.org/10.1038/s41467-018-08229-z.
Johnstone, J.F., Allen, C.D., Franklin, J.F., Frelich, L.E., Harvey, B.J., Higuera, P.E., Mack, M.C., Meentemeyer, R.K., Metz, M.R., Perry, G.L.W., Schoennagel, T., Turner, M.G., 2016. Changing disturbance regimes, ecological memory, and forest resilience. Front. Ecol. Env. 14, 369–378. https://doi.org/10.1002/fee.1311.
Jump, A.S., Ruiz-Benito, P., Greenwood, S., Allen, C.D., Kitzberger, T., Fensham, R., Martínez-Vilalta, J., Lloret, F., 2017. Structural overshoot of tree growth with climate variability and the global spectrum of drought-induced forest dieback. Glob. Change Biol. 23, 3742–3757. https://doi.org/10.1111/gcb.13636.
Kannenberg, S.A., Schwalm, C.R., Anderegg, W.R., 2020. Ghosts of the past: how drought legacy effects shape forest functioning and carbon cycling. Ecol. Lett. 23, 891–901. https://doi.org/10.1111/ele.13485.
Kiorapostolou, N., Petit, G., Dannoura, M., 2019. Similarities and differences in the balances between leaf, xylem and phloem structures in *Fraxinus ornus* along an environmental gradient. Tree Physiol. 39, 234–242. https://doi.org/10.1093/treephys/tpy095.
Kowarik, I., 2023. The Mediterranean tree *Acer monspessulanum* invades urban greenspaces in Berlin. Dendrobiology 89, 20–26. https://doi.org/10.12657/denbio.089.002.
Lemoine, D., Peltier, J., Marigo, G., 2001. Comparative studies of the water relations and the hydraulic characteristics in *Fraxinus excelsior*, *Acer pseudoplatanus* and *A. opalus* trees under soil water contrasted conditions. Ann. Sci. For. 58, 723–731. https://doi.org/10.1051/forest:2001159.
Lloret, F., Lobo, A., Estevan, H., Maisongrande, P., Vayreda, J., Terradas, J., 2007. Woody plant richness and NDVI response to drought events in Catalonian (northeastern Spain) forests. Ecology 88, 2270–2279. https://doi.org/10.1890/06-1195.1.
Lloret, F., Keeling, E.G., Sala, A., 2011. Components of tree resilience: effects of successive low-growth episodes in old ponderosa pine forests. Oikos 120, 1909–1920. https://doi.org/10.1111/j.1600-0706.2011.19372.x.
Nakagawa, S., Johnson, P.C.D., Schielzeth, H., 2017. The coefficient of determination R^2 and intra-class correlation coefficient from generalized linear mixed-effects models revisited and expanded. J. R. Soc. Interface 14. https://doi.org/10.1098/rsif.2017.0213.
Ogle, K., Barber, J.J., Barron-Gafford, G.A., Bentley, L.P., Young, J.M., Huxman, T.E., Loik, M.E., Tissue, D.T., 2015. Quantifying ecological memory in plant and ecosystem processes. Ecol. Lett. 18, 221–235. https://doi.org/10.1111/ele.12399.
Ouyang, S.N., Gessler, A., Saurer, M., Hagedorn, F., Gao, D.C., et al., 2021. Root carbon and nutrient homeostasis determines downy oak sapling survival and recovery from drought. Tree Physiol. 41, 1400–1412. https://doi.org/10.1093/treephys/tpab019.
Pardos, M., Del Río, M., Pretzsch, H., Jactel, H., Bielak, et al., 2021. The greater resilience of mixed forests to drought mainly depends on their composition: analysis along a climate gradient across Europe. For. Ecol. Manage. 481, 118687 https://doi.org/10.1016/j.foreco.2020.118687.
Peltier, D.M., Ogle, K., 2019. Legacies of more frequent drought in ponderosa pine across the western United States. Glob. Chang. Biol. 25, 3803–3816. https://doi.org/10.1111/gcb.14720.
Pignatti, S., 1982. Flora d'Italia. Edagricole, Bologna, Italy.
Pinheiro, J.C., Bates, D.M., 2000. Mixed-Effects Models in S and S-PLUS. Springer, New York.
Portoghesi, L., Chiocchini, U., Dossi, V., Alivernini, A., 2008. Osservazioni geopedologiche e dendrometriche in popolamenti a dominanza di acero trilobo (*Acer monspessulanum* L.) sui Monti della Tolfa (Roma). L'Italia Forestale e Montana 63, 241–257. https://doi.org/10.4129/IFM.2008.3.03.
Poyatos, R., Llorens, P., Piñol, J., Rubio, C., 2008. Response of Scots pine (*Pinus sylvestris* L.) and pubescent oak (*Quercus pubescens* Willd.) to soil and atmospheric water deficits under Mediterranean mountain climate. Ann. For. Sci. 65, 306. https://doi.org/10.1051/forest:2008003.

Pretzsch, H., 2021. Trees grow modulated by the ecological memory of their past growth. Consequences for monitoring, modelling, and silvicultural treatment. For. Ecol. Manage. 487, 118982 https://doi.org/10.1016/j.foreco.2021.118982.

Pretzsch, H., Schütze, G., Uhl, E., 2013. Resistance of European tree species to drought stress in mixed versus pure forests: evidence of stress release by inter-specific facilitation. Plant Biol. 15, 483–495. https://doi.org/10.1111/j.1438-8677.2012.00670.x.

R Development Core Team. R, 2022. A Language and Environment for Statistical Computing. R Foundation for Statistical Computing, Vienna, Austria.

Ripullone, F., Guerrieri, M.R., Nolé, A., Magnani, F., Borghetti, M., 2007. Stomatal conductance and leaf water potential responses to hydraulic conductance variation in Pinus pinaster seedlings. Trees Struct. Funct. 21, 371–378. https://doi.org/10.1007/s00468-007-0130-6.

Rita, A., Camarero, J.J., Nolè, A., Borghetti, M., Brunetti, M., et al., 2020. The impact of drought spells on forests depends on site conditions: the case of 2017 summer heat wave in southern Europe. Glob. Chang. Biol. 26, 851–863. https://doi.org/10.1111/gcb.14825.

Rodell, M., Houser, P.R., Jambor, U., Gottschalck, J., Mitchell, K., Meng, C.J., et al., 2004. The global land data assimilation system. Bull. Am. Meteor. Soc. 85, 381–394. https://doi.org/10.1175/BAMS-85-3-381.

Ruehr, N.K., Grote, R., Mayr, S., Arneth, A., 2019. Beyond the extreme: recovery of carbon and water relations in woody plants following heat and drought stress. Tree Physiol. 39, 1285–1299. https://doi.org/10.1093/treephys/tpz032.

Schwalm, C.R., Anderegg, W.R.L., Mchalak, A.M., et al., 2017. Global patterns of drought recovery. Nature 548, 202–205. https://doi.org/10.1038/nature23021.

Schwarz, J., Skiadaresis, G., Kohler, M., et al., 2020. Quantifying growth responses of trees to drought—a critique of commonly used resilience indices and recommendations for future studies. Curr. For. Rep. 6, 185–200. https://doi.org/10.32942/osf.io/5ke4f.

Sergent, A.S., Rozenberg, P., Bréda, N., 2014. Douglas-fir is vulnerable to exceptional and recurrent drought episodes and recovers less well on less fertile sites. Ann. For. Sci. 71, 697–708. https://doi.org/10.1007/s13595-012-0220-5.

Serra-Maluquer, X., Granda, E., Camarero, J.J., Vilà-Cabrera, A., Jump, A.S., et al., 2021. Impacts of recurrent dry and wet years alter long-term tree growth trajectories. J. Ecol. 109, 1561–1574. https://doi.org/10.1111/1365-2745.13579.

Tissier, J., Lambs, L., Peltier, J.P., Marigo, G., 2004. Relationships between hydraulic traits and habitat preference for six *Acer* species occurring in the French Alps. Ann. For. Sci. 61, 81–86. https://doi.org/10.1051/forest:2003087.

Tomasella, M., Casolo, V., Aichner, N., Petruzzellis, F., Savi, T., Trifilò, P., Nardini, A., 2019. Non-structural carbohydrate and hydraulic dynamics during drought and recovery in *Fraxinus ornus* and *Ostrya carpinifolia* saplings. Plant Physiol. Biochem. 145, 1–9. https://doi.org/10.1016/j.plaphy.2019.10.024.

Tucker, C.J., Sellers, P., 1986. Satellite remote sensing of primary production. Int. J. Rem. Sens. 7, 1395–1416. https://doi.org/10.1080/01431168608948944.

Valeriano, C., Gazol, A., Colangelo, M., Camarero, J.J., 2021. Drought drives growth and mortality rates in three pine species under Mediterranean conditions. Forests 12, 1700. https://doi.org/10.3390/f12121700.

van Kampen, R., Fisichelli, N., Zhang, Y., Wason, J., 2022. Drought timing and species growth phenology determine intra-annual recovery of tree height and diameter growth. AoB Plants 14, plac012. https://doi.org/10.1093/aobpla/plac012.

Vicente-Serrano, S.M., Beguería, S., López-Moreno, J.I., 2010. A multiscalar drought index sensitive to global warming: the standardized precipitation evapotranspiration index. J. Climate 23, 1696–1718. https://doi.org/10.1175/2009JCLI2909.1.

Yin, D., Gou, X., Liu, J., Zhang, D., Wang, K., Yang, H., 2024. Increasing deep soil water uptake during drought does not indicate higher drought resistance. J. Hydrol. 630, 130694.

Yu, X., Orth, R., Reichstein, M., Bahn, M., Klosterhalfen, A., Knohl, A., Koebsch, F., Migliavacca, M., Mund, M., Nelson, J.A., Stocker, B.D., Walther, S., Bastos, A., 2022. Contrasting drought legacy effects on gross primary productivity in a mixed versus pure beech forest. Biogeosciences 19, 4315–4329. https://doi.org/10.5194/bg-19-4315-2022.

Zhang, Y., Keenan, T.F., Zhou, S., 2021. Exacerbated drought impacts on global ecosystems due to structural overshoot. Nat. Ecol. Evol. 5, 1490–1498. https://doi.org/10.1038/s41559-021-01551-8.